

# *Semiconductor properties of manganese dioxide*

E. PREISLER

*Hoechst AG, Werk Knapsack, D 5030 Hürth, near Cologne*

Received 10 July 1975; revised 2 December 1975

Measurements of the d.c. conductivity of different types of  $\gamma$ -manganese dioxide formed under various conditions and of different thermal history indicate a correlation with the combined water content. The specific conductivity increases exponentially as the water content decreases. The values obtained with anhydrous products which then are transformed to a  $\beta$ -manganese dioxide are similar to those obtained with  $\beta$ -manganese dioxide prepared by pyrolysis of manganous nitrate. Any effect which might be attributed to the lattice transformation of  $\gamma$ - into  $\beta$ -manganese dioxide could not be observed.

A more detailed examination of two specimens of manganese dioxide shows a semilogarithmic relation between thermoelectric voltage and d.c. conductivity. This relationship allows an estimate to be made of the electron concentration at which the electron gas would begin to degenerate. Hence it follows that both for  $\gamma$ - and  $\beta$ -manganese dioxide the concentration of the conducting electrons is far below the degeneration limit.

This result is in agreement with the measured activation energies of the conductivity. It is suggested that the water content influences the electronic band structure by successively deforming the rutile structure of  $\beta$ -manganese dioxide and hence the manganese–manganese distances within the lattice.

## 1. Introduction

It has long been known that manganese dioxides are semiconductors. The values of specific conductivity range from  $10^{-6} \text{ ohm}^{-1} \cdot \text{cm}^{-1}$ – $10^3 \text{ ohm}^{-1} \cdot \text{cm}^{-1}$ . As the term manganese dioxide applies to manganese(III)–manganese(IV)-oxides which are to be distinguished with regard to their crystal structure, manganese to oxygen ratio, crystallite size, specific surface, water content, and other properties, the question arises which of these properties have a significant influence on the specific electrical conductivity. The major number of mineralic and artificially prepared manganese dioxides exist in more or less powdery form and can only be measured in the compressed state with or without the application of a pressure during the measurement. The fact that the conductivity depends strongly on the applied pressure clearly shows that the contact resistances between the individual manganese dioxide particles are of decisive importance. An extrapolation to very high pressures is not without problems and so far has not led to the values obtained with block samples of manganese dioxide in the as-grown state [1, 2].

Therefore it seems to be reasonable to restrict the d.c. conductivity measurements to massive samples having densities not too far from the theoretical one. However, suitable test materials are available only to a limited extent. Massive  $\beta$ -manganese dioxide was prepared by Wiley and Knight [3] and by Klose [4] by pyrolysis of manganous nitrate. Its density ranges between  $4.0$ – $4.6 \text{ g cm}^{-3}$ . Landorf and Licht [5] produced thin layers of manganese dioxide having diffuse x-ray reflexions of  $\beta$ - $\text{MnO}_2$  and possibly  $\gamma$ - $\text{MnO}_2$ , by electron sputtering of manganese onto anodized tantalum surfaces. The layers had a density of  $3 \text{ g cm}^{-3}$ . Bhide and Damle investigated the properties of naturally occurring pyrolusite from various sources, some of these samples being massive and possessing crystal orientation [6].

$\gamma$ -phase manganese dioxide of a density of  $4 \text{ g cm}^{-3}$  is on an industrial scale prepared by anodic oxidation of hot and acidic manganese sulphate solutions [cf. e.g., 7]. The  $\alpha$ -variety can be obtained in the presence of potassium ions under analogous conditions [8].  $\gamma$ -manganese dioxides, which exhibit a marked growth orientation and a fibrous structure as well as cleava-

bility, are deposited on the anodes during electrolysis of hot manganous salt solutions in dilute hydrochloric [9], nitric [10], or perchloric [11] acid. Sometimes fibrous, cleavable  $\gamma$ -manganese dioxide also forms in a sulphate bath on anodic oxidation [11]. Very hard, massive  $\gamma$ -manganese dioxide, which is very resistant to fracture, forms in the electrolyte of commercial electrolytic manganese dioxide plants by slow disproportionation and successive hydrolysis of a small manganese(III) content. The material thus obtained has a density of 4.45–4.50 g cm<sup>-3</sup>, which is the highest density of a  $\gamma$ -phase manganese dioxide so far reported [11].

At temperatures within the range of 380 to 420° C the  $\gamma$ -variety is transformed into the  $\beta$ -variety, the density of the starting material being mainly preserved. Therefore the two varieties can be compared directly.  $\gamma$ -phase manganese dioxides always contain combined water, which is set free to an increasing degree as the temperature rises. The thermal treatment is accompanied by a change of the electrical conductivity which has been ascribed among other factors also to the desorption of combined water [12, 13]. Foster, Lee and Tye [14] point out that during the thermal treatment of manganese dioxide powders the surface layers of the particles, whose composition may substantially differ from their bulk composition, considerably affect the results of the measurements. Our experiments were designed to exclude this influence of the surface layers and of the contact resistances on the values of the conductivity. This seems to be necessary for a more

detailed understanding of the important role which is played by the combined water within the crystal structure of  $\gamma$ -manganese dioxide.

## 2. Experimental

### 2.1. Test material

The analytical data for the test materials are given in Table 1. Rectangular samples were cut from EMD and HMD with the aid of a diamond saw. During this operation EMD proved sensitive to fracture, whereas HMD was very hard and could be cut to long and narrow samples. FEMD was split parallel to the direction of growth and then ground to the dimensions desired.

### 2.2. Conductivity measurements

All values of the d.c. conductivity were measured by the four-probe method. The temperature dependence was determined on samples which had been previously heated in air for a period of 12 h at the desired temperature. After this heat treatment the samples were clamped into a sample holder, which on one longitudinal side applies two current leads, and on the opposite side two contacts for the voltage drop measurements, as shown in Fig. 1a. The sample holder was then positioned into a furnace; the free volume was filled with fine sand. A Ni/NiCr thermocouple was positioned near the sample. A constant current of 1 mA was applied to the sample, while the voltage drop and the temperature were recorded by means of an

Table 1. Test materials

Designation*	EMD	FEMD-N	FEMD-S	HMD
Bath	0.75M MnSO <sub>4</sub> 0.7M H <sub>2</sub> SO <sub>4</sub>	0.75M Mn(NO <sub>3</sub> ) <sub>3</sub> 0.6M HNO <sub>3</sub>	0.75M MnSO <sub>4</sub> 0.7M H <sub>2</sub> SO <sub>4</sub>	0.75M MnSO <sub>6</sub> 0.7M H <sub>2</sub> SO <sub>4</sub>
Temperature	95° C	95° C	95° C	95° C
x in MnO <sub>x</sub>	1.95	1.97	1.95	1.98
Combined water	4.2%	4.2%	4.1%	2.4%
Density	4.0 g cm <sup>-3</sup>	4.05 g cm <sup>-3</sup>	3.55 g cm <sup>-3</sup> **	4.45 g cm <sup>-3</sup>
Type of crystal	$\gamma$ -MnO <sub>2</sub>	$\gamma$ -MnO <sub>2</sub>	$\gamma$ -MnO <sub>2</sub>	$\gamma$ -MnO <sub>2</sub>
Growth texture	(+)	+	+	(+)
Cleavage		+	+	—

\* EMD = electrodeposited manganese dioxide

FEMD-N = Fibrous EMD from nitrate bath

FEMD-S = FEMD from sulphate bath

HMD = Hydrolytically deposited manganese dioxide

\*\* FEMD-S powder (particle size 250–500  $\mu$ m) has a pycnometer density of 4.35 g cm<sup>-3</sup>. The compact material has larger cavities.

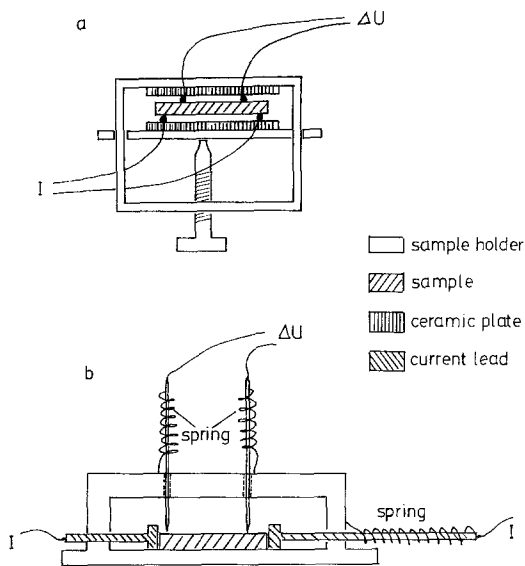


Fig. 1. Apparatus for measuring electrical d.c. conductivity. (a) Measurement of temperature dependence. (b) Measurement at room temperature.

x-y recorder. Only the cooling periods were evaluated, as during the heating period the uniformity of the temperature distribution was not sufficient. The asymmetrical arrangement of the four contacts gave rise to a constant error of about 5–10%.

The dependence of the conductivity on the temperature of heat treatment has been determined by measuring the conductivity only at 25° C. The samples were heat treated at the selected temperature until the change with time of the conductivity was insignificant. The device for the conductivity measurement is described by Fig. 1b. Two current leads are pressed against the front surfaces of the manganese dioxide samples and two needle-like contacts are positioned on the lateral surface. This arrangement ensures in general a uniform current distribution along the cross-section of the sample and a precise distance between the voltage probe contacts. The test current depended on the resistance and ranged between 100  $\mu$ A and 10 mA. Voltage was measured by means of a high-resistance valve voltmeter.

Especially in the case of the fibrous electrolytic manganese dioxide the uniform current distribution is important and can be improved by applying a thin layer of a conductive silver paint on the front surfaces. The FEMD samples consist of bundles of individual fibres arranged parallel to

the large axis of the sample parallelepiped, so that the contact resistances between the fibres cannot be neglected.

Samples that have been heat treated above 400° C were liable to form a thin surface layer of very high ohmic resistivity. This layer has to be removed by slightly polishing the surfaces before the measurement is carried out. This has been done with type 400 silicon carbide grinding paper; the extension of this procedure did not affect the results. Additional samples of approximately the same dimensions and identical thermal history were used for analytical and x-ray diffraction data.

### 2.3. Thermoelectric voltage

The differential thermoelectric voltage was determined at room temperature only. The measuring device is depicted in Fig. 2. A glass tube, having an inner diameter of 5 mm and containing the sample, is slipped onto a copper cylinder of 4.5 mm diameter, which is provided with a small heating coil and serves as a support. Another copper cylinder of the same shape is pressed against the sample by means of a spring (not shown in the figure). The copper cylinders have bore holes of 1.5 mm diameters, into which Ni/NiCr-thermocouples are fitted insulated from the copper by alumina tubes. The thermoelectric voltage is determined as the voltage between the copper cylinders. By applying a controlled current to the heating coil a temperature difference at the ends of the sample was generated and recorded versus the thermoelectric voltage by means of an x-y recorder. Within temperature differences of 10–15° C straight lines are obtained, the slope of which gives the differential thermoelectric voltage. Control measurements on antimony and on nickel are in good agreement with the values reported in the literature.

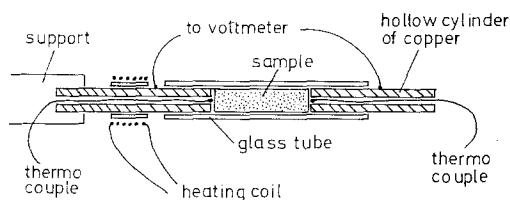


Fig. 2. Apparatus for measuring the differential thermoelectric voltage at room temperature.

## 2.4. Thermogravimetric experiments

Thermogravimetric examination was performed on powdered samples in air. They were heated from 25–750° C at constant heating rates of 2° min<sup>-1</sup> in the case of EMD, HMD and FEMD-N, and of 5° min<sup>-1</sup> in the case of FEMD-S.

## 3. Results

### 3.1. Temperature dependence of d.c. conductivity

All material had been prepared at temperatures between 90 and 95° C. After removal from the bath and cooling to room temperature the materials were designated 'as-grown'. Their conductivity values in this state are given in Table 2.

After heat treatment for 12 h at different temperatures all samples exhibit a temperature dependence of conductivity  $\sigma$  which follows the relation

$$\sigma = \sigma_0 \cdot e^{-(E/kT)} \quad (1)$$

where  $\sigma_0$  is a constant depending on the type of manganese dioxide and the thermal treatment. In  $\log \sigma$  versus  $1/T$ -coordinates Equation 1 will give a straight line. Near the maximum temperature of heat treatment deviations from linearity occur, which probably result from further changes the samples may undergo (Fig. 3).

When the heat treatment temperature is increased, the curves shift to higher values of conductivity while their slopes gradually decrease. The

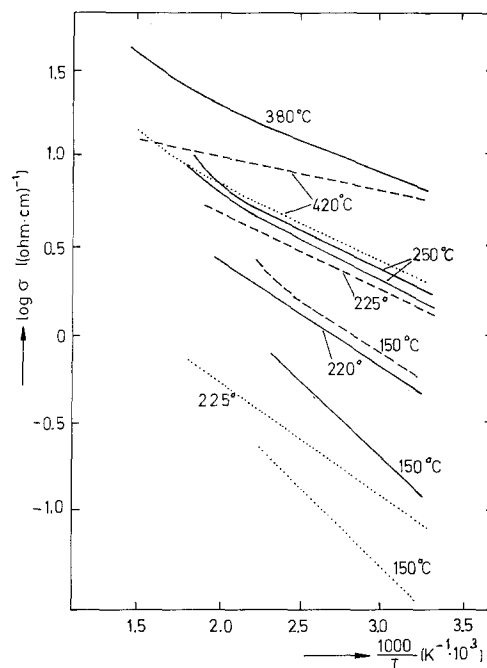


Fig. 3. Temperature dependence of the d.c. conductivity of 'grown' manganese dioxide (FEMD-N: ———, HMD: - - - -, EMD: ····) after heat treatments at indicated temperatures.  $\sigma$  in ohm. cm<sup>-1</sup>.

original differences between HMD and the other types become smaller, which is particularly well demonstrated by comparing the conductivity values at constant temperature, for example at 25° C (Fig. 4). For this set of measurements the samples were subjected to a thermal treatment at a selected temperature for such a time that the

Table 2. Conductivity of solid block manganese dioxide at room temperature

	Literature cited	$\sigma$ (ohm. cm) <sup>-1</sup>	remarks
Bhide and Damle	6	0.1	naturally occurring compact pyrolusite
Wiley and Knight	3	6.6	D = 4 g cm <sup>-3</sup> , $\beta$ -MnO <sub>2</sub>
Landorf and Licht	5	2–5	D = 3 g cm <sup>-3</sup> , thin film, $\beta$ -MnO <sub>2</sub>
Klose	4	300	D = 4.7 autoclave- $\beta$ -MnO <sub>2</sub>
		10	D = 4.0 g cm <sup>-3</sup> , $\beta$ -MnO <sub>2</sub>
Amano <i>et al.</i>	9	0.008–0.14	FEMD from chloride bath, $\gamma$ -MnO <sub>2</sub>
		0.006	non-fibrous EMD, $\gamma$ -MnO <sub>2</sub>
This paper		0.008–0.03	EMD, Data see Table 1
		0.01–0.1	FEMD-N, parallel to the direction of growth*
		0.01	FEMD-S
		0.2–0.5	HMD

\* Conductivity data obtained by measuring in the direction normal to the direction of growth were always lower by a factor of 3–4. This is presumably due to contact resistances between the individual fibres of this material. For this reason it is not possible to draw any conclusions on lattice anisotropy of the conductivity.

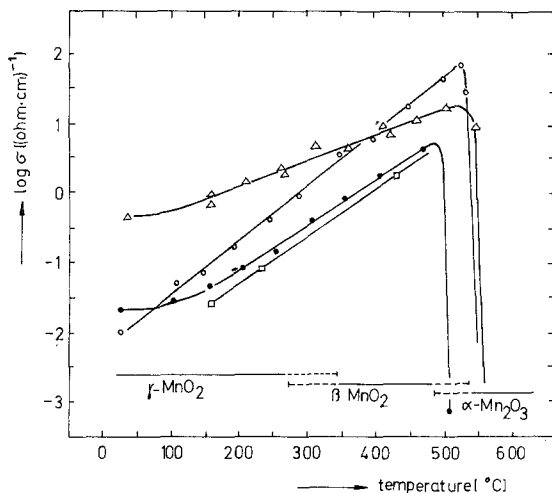


Fig. 4. Specific electrical conductivity  $\sigma$  as a function of the temperature  $T$  of the heat treatments of various types of manganese dioxide.  $\Delta$ : HMD;  $\circ$ : FEMD-N;  $\bullet$ : FEMD-S;  $\square$ : EMD. Measurements carried out at 25° C. Ranges of occurrence determined by x-ray technique: — single-phase; - - - two-phases. Degrees of oxidation ( $x$  in  $\text{MnO}_x$ ): 25° C and 100° C: 1.95; 350° C: 1.93; 400° C: 1.92; 450° C: 1.90.  $\sigma$  in  $\text{ohm}^{-1}\cdot\text{cm}^{-1}$ .

change in the conductivity values became insignificant. This implies treatment times of 12 h at temperatures about 100–200° C, or of 1–2 h at 400–500° C. Hence it follows that the state of a sample cannot be defined by a heat treatment temperature alone, but has to be characterized by additional parameters such as the degree of oxidation and composition.

At temperatures within the range of 100–500° C all four types of manganese dioxide fit well into the equation

$$\log \sigma_{25} = A \cdot T^* + B \quad (2)$$

where  $\sigma_{25}$  = conductivity at 25° C,  $T^*$  = temperature of heat treatment,  $A$  and  $B$  = constants.  $A$  and  $B$  are practically identical for EMD and FEMD-S, both of which were deposited from sulphate baths.

During heat-treatment at increasing temperatures  $\gamma$ -manganese dioxide undergoes a transformation to  $\beta$ -manganese dioxide and then a decomposition to  $\alpha$ -manganese(III) oxide. The temperature regions of existence of these compounds as determined by x-ray diffraction with FEMD-N samples are given in Fig. 4. The dashed lines indicate regions of transition.

The linearity between  $\log \sigma_{25}$  and  $T^*$  shows that the differences in the lattice structure of  $\gamma$ -

and  $\beta$ -manganese can at best have a slight effect on the electron conductance mechanism. Transformation to  $\beta$ - $\text{MnO}_2$  might be expected to alter the slope or to introduce a discontinuity into the  $\log \sigma$  versus  $T$  plot.

Furthermore it can be seen that likewise the slight change in the degree of oxidation (defined as  $x$  in the formula  $\text{MnO}_x$ ) which at temperatures between 300 and 450° C decreases from 1.95–1.90 does not lead to any inflection of the curves of Fig. 4. Even the first appearance of  $\alpha$ - $\text{Mn}_2\text{O}_3$  at a temperature of 475° C does not yet lead to a change of the slope, although the conductivity of pure  $\alpha$ - $\text{Mn}_2\text{O}_3$  is lower by about 6 orders of magnitude. Maybe the formation of incoherent regions of  $\alpha$ - $\text{Mn}_2\text{O}_3$  phase which are statistically distributed in the  $\beta$ - $\text{MnO}_2$  matrix has no other effect than that of a decrease in the effective density of  $\beta$ -manganese dioxide.

### 3.2. Water content and conductivity

Only a small percentage of water present in electrodeposited manganese dioxide is volatile at 120° C. The predominant portion of it is desorbed in a relatively smooth manner during temperature programmed heating (Fig. 5). At temperatures above 300–350° C the desorption of water is superimposed by a slow loss of oxygen, which at temperatures up to 350° C amounts to 0.7% by weight. The values of water content determined by direct chemical analysis of FEMD-N samples of the same history corresponded quite satisfactorily with the values determined by TGA.

Whereas at temperatures around 300° C the decomposition of manganese dioxide takes place slowly and is mainly restricted to regions near the surface (formation of highly resistive surface layers, a phenomenon also observed by Foster, Lee and Tye [14] in evaluating measurements of the impedance of heat-treated EMD powders), manganese dioxide undergoes very rapid decomposition at temperatures above 530° C (the steep steps in the T.G.A. curves). The water content seems to be of structural necessity to the  $\gamma$ -modification. It may, however, be considerably reduced, before the  $\beta$ -modification appears. HMD does not lose any water up to 120° C; its total water content amounts to 2.4%, and this is much lower than that of EMD.

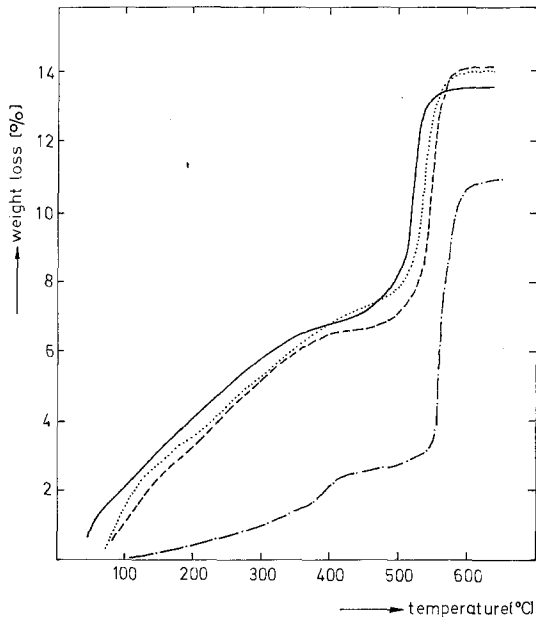


Fig. 5. Thermogravimetric decomposition of various types of manganese dioxide. —: FEMD-S; - - -: FEMD-N; ····: EMD; - · - ·: HMD. Heating speed  $5^{\circ}\text{C min}^{-1}$  for FEMD-N, EMD and HMD;  $2^{\circ}\text{C min}^{-1}$  for FEMD-S.

The correlation between the water content and the electrical conductivity at  $25^{\circ}\text{C}$  now fit comparatively well into a logarithmic dependence. The  $\log \sigma_{25}$  versus  $c_{\text{H}_2\text{O}}$  curves for all four types of manganese dioxide are fairly close to each other, which is surprising with regard to the conductivity values of the 'as-grown' sample of HMD. This fact suggests a significant importance of the water content of  $\gamma$ -manganese dioxide on the mechanism of the electric conductivity (Fig. 6).

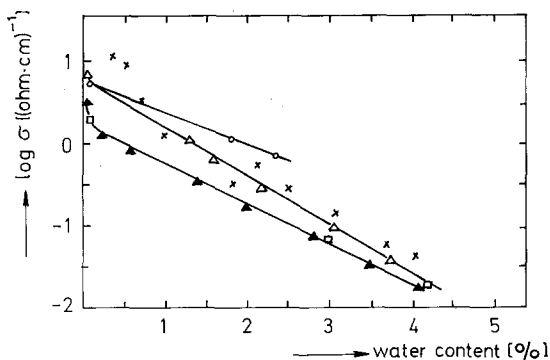


Fig. 6. Relation between the water content of various types of manganese dioxide and their specific conductivity at room temperature.  $\square$ : EMD;  $\blacktriangle$ : FEMD-S;  $\triangle$ : FEMD-N;  $\circ$ : HMD;  $\times$ : FEMD-N, water content determined directly.  $\sigma$  in  $\text{ohm}^{-1}\cdot\text{cm}^{-1}$ .

### 3.3. Activation energy of the conductivity

The activation energy for conduction was calculated on the basis of the measurements shown in Fig. 3. For the samples, which had been heat-treated until their water content was near zero, the activation energies were found to be between 0.04 and 0.10 eV, whereas the values for the original samples range between 0.09 and 0.20 eV for HMD and EMD, respectively. Fig. 7 shows the dependence of the activation energy on the level of conductivity on a logarithmic scale for FEMD-N, EMD, and HMD. Data after the results of Klose [4] are added to show analogous values for a  $\beta$ -manganese dioxide, which had been prepared by thermal decomposition of manganous nitrate. The activation energy is higher the lower the conductivity, no matter whether the conductivity change is due to the incorporation of water or to the nonstoichiometric composition of the  $\beta$ -phase manganese dioxide.

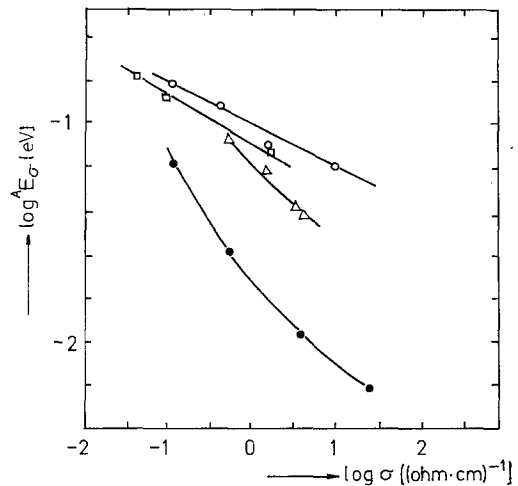


Fig. 7. Activation energies  $A E_{\sigma}$  as a function of the d.c. conductivity  $\sigma$  at  $25^{\circ}\text{C}$ .  $\square$ : EMD;  $\circ$ : FEMD-N;  $\triangle$ : HMD;  $\bullet$ : according to results of measurements on  $\beta\text{-MnO}_2$  obtained by Klose [4] (products prepared in an autoclave, cf. text).

### 3.4. Differential thermoelectric voltage

All  $\gamma$ -manganese dioxide types exhibit a negative thermoelectric voltage  $\phi$  in agreement with the literature. They are therefore regarded as n-type semiconductors. Within the temperature range of heat-treatment of  $100^{\circ}$  to about  $250^{\circ}\text{C}$  no

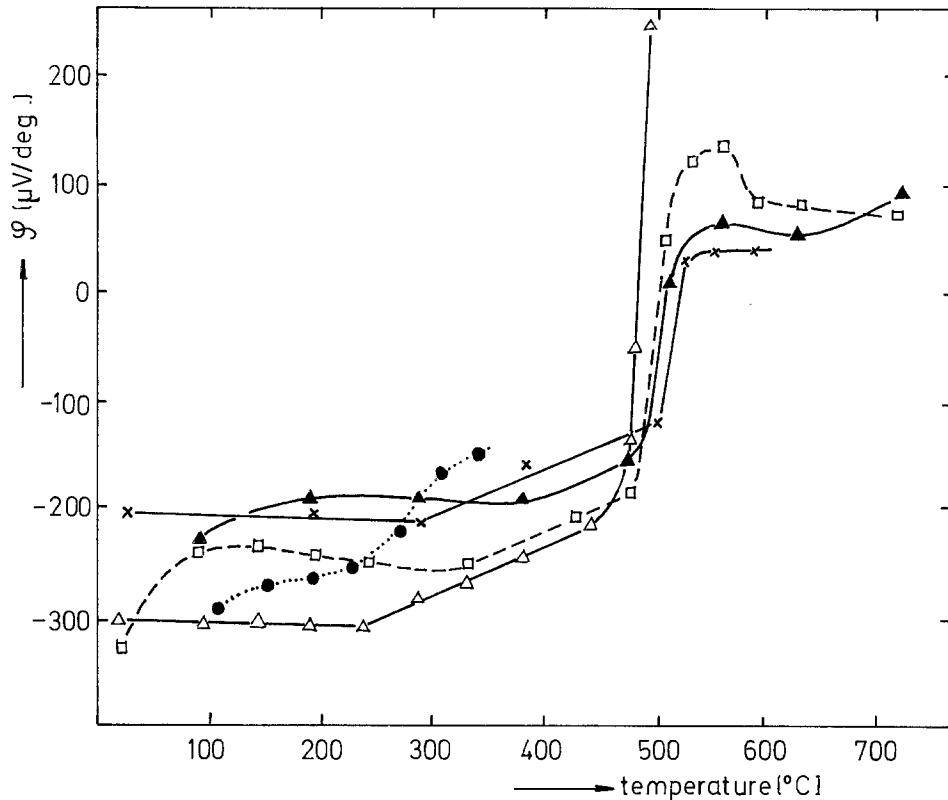


Fig. 8. Differential thermoelectric voltage  $\phi$  as a function of the temperature  $T^*$  of the heat treatments of various types of manganese dioxide.  $\phi$  measured at 25°C.  $\blacktriangle$ : EMD;  $\triangle$ : FEMD-S;  $\square$ : FEMD-N;  $\times$ : HMD;  $\bullet$ : according to measurements carried out on EMD powder by Foster, Lee and Tye [14].

clear relationship between thermoelectric voltage and heating temperature can be observed. The values tend to scatter by up to  $\pm 30 \mu\text{V deg}^{-1}$ . At higher temperatures the scattering is reduced to  $\pm 7 \mu\text{V deg}^{-1}$ . In this region the thermoelectric voltage becomes less negative with increasing heat-treatment temperature. A sharp rise to positive values is connected with the formation of  $\text{Mn}_2\text{O}_3$  (Fig. 8).

The relation between d.c. conductivity and differential thermoelectric voltage of FEMD-N and FEMD-S has been examined (Fig. 9). In both cases there is a semilogarithmic relation between these two properties. In Fig. 9 a similar curve is given, too, which results from the evaluation of measurements performed by Foster, Lee and Tye [14] on EMD powders that had been outgassed and subjected to thermal treatments at various temperatures.

According to the elementary semiconductor theory the differential thermoelectric voltage of an n-type semiconductor is given by

$$\phi = \frac{k}{e} \left( A - \ln \frac{n}{n^0} \right) \quad (3)$$

and its electrical conductivity by

$$\sigma = e\mu_n n \quad (4)$$

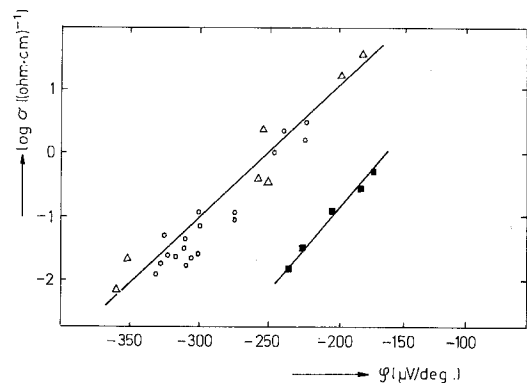


Fig. 9. Conductivity  $\sigma_{25}$  as a function of the thermoelectric voltage of heat treated manganese dioxide.  $\phi$  measured at 25°C.  $\triangle$ : FEMD-N;  $\circ$ : FEMD-S;  $\blacksquare$ : according to measurements carried out by Foster, Lee and Tye [14] on EMD powder. — regression line.

where  $n$  = concentration of the conducting electrons per unit volume,  $n^0$  = concentration of electrons in the conduction band at which the electron gas begins to degenerate (the semiconductor behaves as a metal),  $\mu_n$  = mobility of the conductive electrons,  $e$  = charge of the electron,  $k$  = the Boltzmann constant,  $A$  = constant.  $A$  depends on the Debye temperature of the compound and ranges between 2.5 and 4 for ionic lattices. As

	$\phi$ (V deg <sup>-1</sup> )	$\sigma$ (ohm <sup>-1</sup> .cm <sup>-1</sup> )	$\mu_n^*$ (cm <sup>2</sup> /V.s)	$n$ (cm <sup>3</sup> )	$n^0$ (cm <sup>3</sup> ) $A = 3$	$A = 4$
$\gamma$ -MnO <sub>2</sub>	$3.5 \times 10^{-4}$	$10^{-2}$	4.2	$1.5 \times 10^{16}$	$7.5 \times 10^{21}$	$4.3 \times 10^{21}$
$\beta$ -MnO <sub>2</sub>	$2.0 \times 10^{-4}$	10	21	$3 \times 10^{18}$	$0.9 \times 10^{21}$	$0.4 \times 10^{21}$

\*From measurements of the Hall voltage on  $\beta$ -MnO<sub>2</sub> samples of the same conductivity according to Klose [4].

manganese dioxide has no melting point, one might estimate the Debye temperature of MnO<sub>2</sub> by using the melting temperature of the isostructural titanium dioxide (2100 K). Then the Debye temperature is found to be about 250 K, which is lower than the experimental temperature. Therefore  $A$  may be near 3.

From Equations 3 and 4 it follows that

$$\phi = \frac{k}{e} \left( A - \ln \frac{\sigma}{e\mu_n n^0} \right) \quad (5)$$

$$\phi = -2.0 \times 10^{-4} \log \sigma + 2.0 \times 10^{-4} \times \left( \log e\mu_n n^0 + \frac{A}{2.3} \right) \quad (6)$$

where  $\phi$  is V degree<sup>-1</sup> and  $\sigma$  ohm<sup>-1</sup>.cm<sup>-1</sup>. The differentiation of Equation 6 leads to

$$\frac{d\phi}{d \log \sigma} = -2 \times 10^{-4} \quad (7)$$

e.g. if  $\mu_n n^0$ , the product of mobility and degeneration concentration, is constant, the relation between  $\phi$  and  $\log \sigma$  should be a straight line with the slope of  $-2 \times 10^{-4}$ . The presupposition of constancy of this product seems fairly well realized (Fig. 9). However, the slope of that line, which amounts to  $0.5 \times 10^{-4}$  for FEMD-N and FEMD-S likewise and to  $0.38 \times 10^{-4}$  for EMD powders (according to the data extracted from the work of Foster, Lee and Tye [14]) deviates considerably from the theory.

Equation 6 can be used to estimate the degener-

ation concentration of the conductive electrons. The deviation of the experimental coefficients from the theoretical ones is taken into consideration by replacement of  $(k/e)$  by  $0.25(k/e)$ . The question whether this replacement will be valid also for the second term of Equation 6 cannot be decided. From Equations 4 and 6 one can now calculate values of  $n$  and  $n^0$  for  $\gamma$ -MnO<sub>2</sub> and  $\beta$ -MnO<sub>2</sub>, prepared by heat-treatment of  $\gamma$ -MnO<sub>2</sub>:

Hence it follows that the carrier concentration in the conduction band of  $\beta$ -phase manganese dioxide is smaller than the degeneration concentration  $n^0$  by two orders of magnitude. This implies that there is no metallic conduction. The degeneration concentration of  $\gamma$ -phase manganese dioxide is approximately the same as that of the  $\beta$ -phase. The carrier concentration, however, is much below that of  $\beta$ -manganese dioxide. J. N. Das found a carrier concentration of  $\sim 4.3 \times 10^{19}$  cm<sup>-3</sup> for solid pyrolusite samples [23].

#### 4. Discussion of the results

The examination carried out on solid manganese dioxide having a high density clearly shows that the semiconductor properties are affected by at least two different factors. Departing from stoichiometric  $\beta$ -manganese dioxide the partial reduction by thermal splitting off of oxygen causes a decrease of the conductivity while the activation energy increases [4]. The generation of oxygen vacancies reduces the carrier concentration in the conduction band, the vacancies acting probably as electron scattering centres. A quantitative treatment of this effect is dependent on the preparation of largely homogeneous single phase manganese dioxides having decreasing degrees of oxidation. Owing to the small phase interval of homogeneity of  $\beta$ -manganese dioxide,  $\alpha$ -manganese(III) oxide soon forms during heat-treatment as a new, distinct phase, so the range of investigation is rather limited.



The second factor is considered to be the content of combined water in  $\gamma\text{-MnO}_2$  or any property which is closely related to it. By the term 'combined water' we understand that content of water whose separation kinetics is independent of the partial vapour pressure of the ambient atmosphere, as was shown by Lee, Newnham and Tye [15]. Although the binding state of the water is not uniform and it is difficult to determine that portion which is present in the lattice in the form of  $\text{OH}^-$  ions, the d.c. conductivity is affected by the water content in a surprisingly systematic manner.

To understand the exponential dependence of  $\sigma$  on the content of combined water, one can visualize that part of water which is bound in the lattice as  $\text{OH}^-$  groups partially attached to  $\text{Mn}^{3+}$  ions and partially to  $\text{Mn}^{4+}$  ions as acting as scattering centres in about a similar way as oxygen voids. But an increasing concentration of scattering centres should produce a linear decrease of the conductivity if we do not accept an activation energy distribution for the scattering centres. In this case, perhaps, the rule of Meyer and Neldel [c.f. 21] could be applied, which is given by Equation 8:

$$\Delta E_n = \Delta E_0 - \alpha \log \sigma \quad (8)$$

where  $\Delta E_n$  is the activation energy of the  $n$ th. impurity energy level and  $\Delta E_0$  and  $\alpha$  are constants. But it seems difficult to treat  $\text{OH}^-$  groups in the same way as the usual metallic impurities in semiconductors.

Furthermore, a comparison of the  $\text{OH}^-$  group concentration per unit volume and the concentration of free carriers in  $\gamma$ -manganese dioxide shows that only a small part of the combined water could act as such an impurity. If we assume that the combined water is present mainly as  $\text{OH}^-$  groups, then we find the number of  $\text{OH}^-$  groups in manganese dioxide having a water content of only 1% to be  $N_{\text{OH}} = 2.68 \times 10^{21} \text{ cm}^{-3}$ . This value is, however, by about 2 orders of magnitude, greater than the carrier concentration in  $\beta\text{-MnO}_2$ . Hence it follows that if all  $\text{OH}^-$  groups were such activable centres, very low contents of OH groups would have to lead to a marked decrease in conductivity.

The validity of the  $\log \sigma$  versus  $c_{\text{H}_2\text{O}}$  relation up to 4%  $\text{H}_2\text{O}$  excludes the assumption that only a very small part of the combined water may be

responsible for the large conductivity changes. From this it also follows that the water content of  $\gamma$ -manganese dioxide must play an important role within the crystal structure. Electrodeposited manganese dioxide having, for example, the typical composition  $\text{MnO}_{1.96} \cdot 0.23\text{H}_2\text{O}$  (water content after drying for 2 h at  $120^\circ \text{C}$ ) accordingly contains 0.46 moles of  $\text{OH}^-$  groups per mole of manganese, if we assume that all of this water is bound in the form of  $\text{OH}^-$  groups. Even if the content of  $\text{Mn}^{3+}$  is compensated by 0.08 moles of  $\text{OH}^-$  groups, there are still 0.17 moles of  $\text{Mn}^{4+}$  ions to which two  $\text{OH}^-$  groups would have to be attached. An analogous calculation for HMD with its lower content of combined water reveals two  $\text{OH}^-$  groups to every eighth  $\text{Mn}^{4+}$  ion. For this reason the attempt to explain the crystal structure of  $\gamma$ -manganese dioxide by mere combination of  $[\text{MnO}_6]$ -octahedra to linked chains of the ramsdellite and pyrolusite type (intergrowth structure [17, 18]) seems to be unsatisfactory.

A proposal, which takes into account the lattice structure, is made by Freund [19] and is based on the assumption that the electrons are transported by a hopping mechanism consisting of the tunneling of an electron from one manganese orbital to the next neighbour manganese orbital. The probability  $D$  of tunneling of an electron with the kinetic energy  $E$  through a potential barrier, having the barrier height  $U$  and basic length  $a$ , is given by

$$D = \left( \frac{4\lambda}{\lambda^2 + 1} \right)^2 e^{-2\kappa a} \quad (9)$$

or

$$\ln D - 2 \ln \left( \frac{4\lambda}{\lambda^2 + 1} \right) = -2\kappa a \quad (9a)$$

where  $\lambda = \kappa/k$ ;  $\kappa^2 = (2m/\hbar^2)(U - E)$ ;  $k^2 = (2m/\hbar^2)E$ ; and  $m$  = mass of the electron,  $\hbar$  = Planck's quantum,  $\hbar = h/2\pi$ . Equations 9 and 9a applies for  $\kappa \gg 1$ , that is for the case where the energy of the electron is significantly lower than the barrier height [22]. Equation 9a shows that  $\ln D$  decreases linearly with increasing distance of two corresponding manganese atoms. The d.c. conductivity will therefore decrease if the manganese-manganese distance becomes enlarged by a lattice extension in the current direction caused by the incorporation of additional oxygen in form of  $\text{OH}^-$  groups. X-ray diffraction analysis of FEMD-N suggests a crystal structure of  $\gamma$ -manganese

dioxide which is in agreement with this explanation and which will be reported elsewhere [20].

If on heating hydroxyl groups become detached, domains of the pyrolusite structure randomly distributed within the sample will appear. It has shorter Mn–Mn distances possessing increased tunneling probability and therefore increased conductivity. The amount of the pyrolusite domains will linearly increase with decreasing hydroxyl group content of the manganese dioxide sample, so that a correlation between water content and conductivity of that type given in Fig. 6 will be reasonable.

### Acknowledgement

The author wishes to thank the Head of Research of Hoechst A.G. for the permission to publish this paper, Dr E. G. Schlosser, Hoechst, for helpful discussions concerning the interpretation of the results, and Dr J. A. Lee, London, for correcting the English manuscript.

### References

- [1] K. J. Euler, *Bull. ASE* **63** (1972) 1498.
- [2] *Idem*, *Metalloberfläche, Angew. Elektrochem.* **28** (1974) 15.
- [3] J. S. Wiley and H. T. Knight, *J. Electrochem. Soc.* **111** (1964) 656.
- [4] P. H. Klose, *Ibid* **117** (1970) 854.
- [5] R. W. Landorf and S. J. Licht, *Ibid* **119** (1972) 430.
- [6] V. G. Bhide and R. V. Damle, *Physica* **26** (1960) 33.
- [7] K. Takahashi, in K. Takahashi, S. Yoshizawa and A. Kozawa, (Eds.), 'Electrochemistry of Manganese Dioxide and Manganese Dioxide Batteries in Japan', Vol. II, pp. 23 *et seq.*, The US-Branch Office, The Electrochem. Soc. of Japan (1971).
- [8] E. Preisler, H. Harnisch and G. Mietens, German patent specification no. 2026597 (May 30, 1970) (Knapsack A.G.).
- [9] Y. H. Amano, H. D. Kumano, A. N. Nishino, and Y. M. Noguchi, German patent nos. 1592466 and 1796303 (Dec. 19., 1967), (Matsushita Electric Ind., Co, Ltd).
- [10] Matsushita Electric Ind. Co., Ltd., Jap. patent 7235677 (Nov. 5, 1968).
- [11] E. Preisler, *J. Appl. Electrochem.* **6** (1976) 301.
- [12] K. Sasaki and K. Kojima, *J. Electrochem. Soc. Japan* **22** (1954) 564.
- [13] J. Brenet, *Croatica Chemica Acta* **44** (1972) 115.
- [14] I. B. Foster, J. A. Lee and F. L. Tye, *J. Appl. Chem. Biotechnol.* **22** (1972) 1085.
- [15] J. A. Lee, C. E. Newnham, F. S. Stone and F. L. Tye, *Colloid and Interface Sci.* **42** (1973) 372, *ibid.* **45** (1973) 289.
- [16] J. Brenet, *J. Chem. Ing. Techn.* **38** (1966) 658.
- [17] P. M. De Wolff, *Acta Cryst.* **12** (1959) 341.
- [18] A. M. Byström, *Acta Chem. Scand.* **3** (1949) 163.
- [19] F. Freund, private communication.
- [20] F. Freund, Elisabeth Könen and E. Preisler, Proceedings 'Manganese Dioxide Symposium', Vol. I, No. 16, J.G. Sample Office, Union Carbide Corp., Cleveland, Ohio (1975).
- [21] A. F. Joffé, 'Physik der Halbleiter', Akad. Verl., Berlin, 1960, pp. 136–7.
- [22] S. Flüge, 'Rechenmethoden der Quantentheorie', Springer Verl., Berlin 1965, S. 40).
- [23] J.N. Das, *Z. Phys.* **151** (1958) 345.